applied sciences

MDPI

Article

The FEM Model of the Pump Made of Dielectric Electroactive Polymer Membrane

Jakub Kołota

Institute of Automatic Control and Robotic, Faculty of Control, Robotics and Electrical Engineering, Poznan, University of Technology, 60-965 Poznań, Poland; Jakub.Kolota@put.poznan.pl; Tel.: +48-6166-5-2504

Received: 9 March 2020; Accepted: 25 March 2020; Published: 27 March 2020

check for updates

Abstract: Dielectric electroactive polymers (DEAPs) undergo large deformations when subject to an electric field, which make them an attractive material for use in novel actuator systems. This article presents the possibility of using DEAPs to model an innovative pumping actuator structure. The model was used to map important object parameters at individual operating points of the modeled pump. The experimental work involved designing the membrane and testing its changes in elasticity under the influence of varying forces and voltage supplies. In the further part of the work, a finite element model (FEM) of a pumping device was implemented. In the new construction of the pump, pressure is generated by membrane deformation. This is due to electrostatic compressive force between two electrodes applied to the polymer surface and forces generated by permanent magnets. The results are presented graphically, confirming the compliance of the model with the measurements.

Keywords: DEAP; FEM; dielectric electroactive polymers; finite element method

---

1. Introduction

Smart materials are ones that can change their properties in a controlled manner in response to environmental stimuli. Such materials can be used both as sensors and actuators [1,2]. Electroactive materials like DEAPs (dielectric electroactive polymers) are included in the group of smart materials and are increasingly used in many automation and robotics systems [3]. This work presents the concept of a device using an electroactive polymer that changes its mechanical properties under the influence of voltage excitation.

Finite element model (FEM) modeling of the behavior of DEAPs is a useful tool to understand such systems better and help in the optimal design of prototypes. The modelling and simulating of DEAP actuators is a cost-effective way of providing a better understanding of the devices built with their usage. DEAPs offer excellent performance, are lightweight, flexible and inexpensive. Therefore, dielectric elastomers, provide many potential applications as micro-actuators. A technique to accurately model this material—taking into account its nonlinearities as well as its large deformations—is being developed in this study. This work presents a model of the innovative construction of the pump using DEAP membrane deformation.

There are many works that describe different modeling methods and analytical models [4]. One of the works presents a technique for accurate modeling of electroactive polymer taking into account nonlinearities and large deformations [5]. The authors simulated an algorithm in the ANSYS environment that considers the electromechanical coupling of the EAP (electroactive polymers) model. Simulation of charge distribution and electrostatic force is the subject of another work which uses COMSOL software [6]. Another work focuses on studying the kinematics of forming and loading, along with thermodynamics [7]. While much theoretical and computational modeling effort has gone into describing the ideal, time-independent behavior of these materials, viscoelasticity is a crucial component of the observed mechanical response, and hence has a significant effect on electromechanical actuation. In [8], the authors show that viscoelasticity provides stabilization that delays the onset of instability under monotonic loading and may fully suppress instabilities under sufficiently fast cyclic loading, which may be desirable for many applications. Although all of these models provide advantageous insights into the behavior of the elastomer material, they lack the ability to accurately predict the complete DEAP actuator structure. They focus on several aspects of modeling but are not able to reflect the full complexity.

In this work, an FEM model was made that was verified faithfully with measurements. First, the relationship between static deformation and applied force was presented. Next, three series of displacement measurements were compared for a given force during alternating voltage applied to the membrane. The results prepared in this way allowed us to identify the values of the virtual Young's modulus corresponding to individual points of states by collecting a sufficient number of real object measurements. Using the work state mapping method, it was possible to model devices with sufficient precision having the knowledge how the membrane will deform; it was not necessary to calculate the full complexity of the model each time.

2. Principle of Operation of DEAP Actuator

A DEAP membrane is made of a silicone membrane that is pre-stretched during the production process. Then, the carbon grease electrodes are printed. In principle, DEAPs are similar to flexible capacitors. As can be seen in the Figure 1, they consist of an elastomeric film sandwiched between two electrodes. Applying voltage to them leads to compression of the elastomer, which causes a change in capacity [9–13].

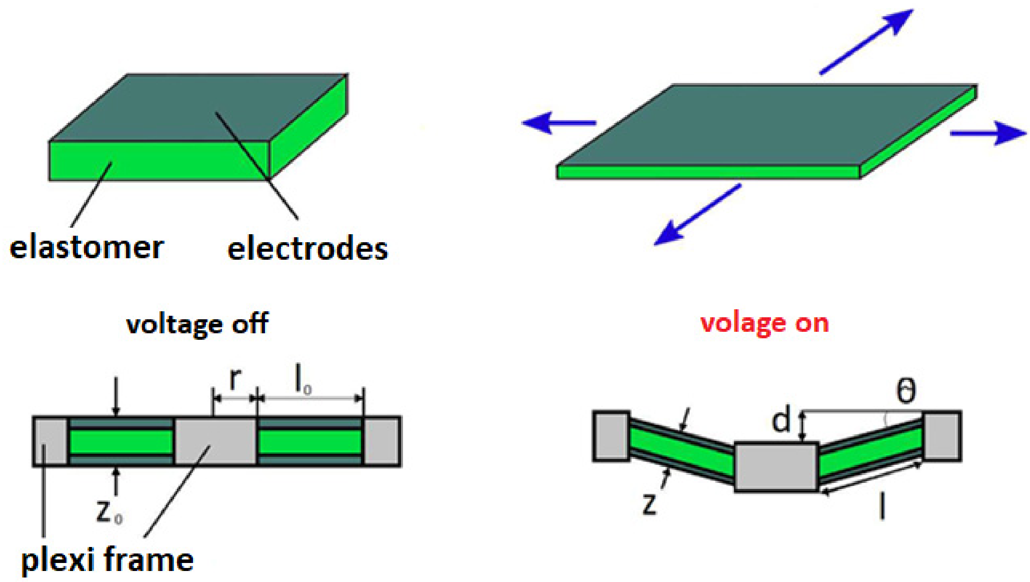

Figure 1. Principle of operation of dielectric electroactive polymer actuator

For this circular geometry, the deflection of the DEA membrane is described by the radial stretch λ_r, circumferential stretch λ_c and thickness stretch λ_z [14].

$$\lambda_r \lambda_c \lambda_z = 1 \quad \lambda_r = \frac{l}{l_0} = \frac{\sqrt{l_0^2+d^2}}{l_0} \quad \lambda_z = \frac{z}{z_0} \quad \lambda_c = const \tag{1}$$

$$z = z_0 \frac{l_0}{l} = z_0 \frac{l_0}{\sqrt{l_0^2+d^2}} \quad \sin(\theta) = \frac{d}{\sqrt{l_0^2+d^2}} \tag{2}$$

I propose a dynamic model composed of a set of nonlinear, time-invariant differential equations describing the dynamic relationship between the input voltage u and the output actuator displacement

d. I present a model which accurately describes the behavior of the actuator, both in transient and steady state, and for different mass loads. The vertical force equilibrium causing membrane deformation can be defined as:

$$m\ddot{d} = mg + F_L - sin(\theta)\left(F_M + F_h + F_f\right) \tag{3}$$

where d is a distance, θ is an angle, m is the mass of the initial load, g means standard gravity and F_L defines the external load. The electromechanical coupling is produced by Maxwell Stress which compresses the membrane when a voltage u is applied to the DEAP. The actuation is in the thickness direction and due to constant volume produces the change of radial stretch y_r. The value of F_M is equal to:

$$F_M sin(\theta) = \overline{c_1} c_2 d u^2 \tag{4}$$

$$\overline{c_1} = \frac{2\pi r z_0}{l_0},\ \overline{c_1} = -\frac{\varepsilon_0 \varepsilon_r}{z_o^2} \tag{5}$$

where ε_0 is vacuum permittivity and ε_r is the relative permittivity of the polymer material. The parameters z_0, l_0 and r describe the geometry of DEAP actuator and are defined in Table 1. Force F_u considers dynamic viscoelastic process according to:

$$F_h sin(\theta) = \overline{c_1} d \sigma_e \left(\frac{l_0^2}{l_0^2 + d^2}\right) \tag{6}$$

$$\sigma_e = -k_e \epsilon_e + k_e(\lambda_r - 1) + \underline{\sigma_e} \tag{7}$$

$$\dot{\epsilon_e} = -\frac{k_e}{\eta_e}\epsilon_e + \frac{k_e}{\eta_e}(\lambda_r - 1) \tag{8}$$

Table 1. DEAP actuator model parameters.

Parameter	Symbol	Value	Unit
mass	m	125	g
standard gravity	g	9.81	m/s^2
vacuum permittivity	ε_0	8.85*10^{-12}	F/m
relative permittivity	ε_r	8.73	-
coefficient of viscoelasticity	k_e	3.11	MPa
coefficient of viscoelasticity	η_e	13.4	MPa·s
damping coefficients	b	1.45	Nms
Ogden model coefficients	β_1	11.4	kPa
Ogden model coefficients	β_2	50.3	kPa
Ogden model coefficients	β_3	44.1	kPa
Ogden model coefficients	γ_1	−118	kPa
Ogden model coefficients	γ_2	−30.4	kPa
Ogden model coefficients	γ_3	23.3	kPa

There are many hyperelastic strain energy density functions, such as Yeoh, Ogden, Arruda-Boyce, etc. Similar to [11], I use the Ogden model and define two parameters β_i and γ_i to obtain to the expression for the hyperelastic stress σ_e:

$$\underline{\sigma_e} = \sum_{i=1}^{3}\left(\beta_i \lambda_r^{\alpha i} - \gamma_i \lambda_r^{-\alpha i}\right) \tag{9}$$

where α_i is 2, 4 and 6. The main difficulty encountered with the identification of the DEAP parameters in the dynamic case is to obtain the damping coefficients b and the coefficients of the viscoelastic k_e and

η_e. In this case the optimization procedure is based on both a step response and a frequency response (the results of this work were published in the [15,16]). Viscous friction is defined as:

$$F_f sin(\theta) = b\dot{\lambda}_r sin(\theta) = \frac{b\dot{d}d^2}{l_0^3 + l_0 d^2} \tag{10}$$

where b is damping coefficient.

3. Experiments

3.1. Static Characteristics

In order to develop a faithful mathematical model, it was necessary to obtain real device parameters by measuring and identification process. Figure 2 presents the laboratory set used to collect displacement measurements depending on the static force acting on the DEAP membrane. The laboratory set contained a high voltage amplifier TREK MODEL 10/10B-HS, laser distance sensor Micro-Epsilon optoNCDT ILD1320–10 with 1 µm accuracy and an Inteco RT-DAC/USB data acquisition card. The actuator presented in our research was made of 3M VHB tape which was pre-stretched during the production process (1 mm to 200 µm thickness). The dimensions of the actuator created by the author are presented in detail in Table 2.

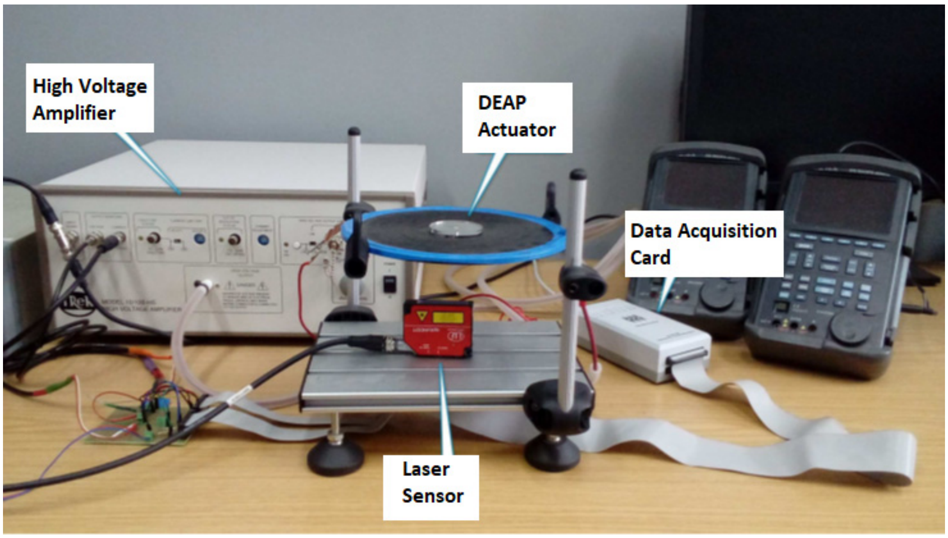

Figure 2. The laboratory kit with dielectric electro active polymer actuator.

Table 2. Dimensions of dielectric electroactive polymer actuator.

Parameter	Symbol	Value	Unit
Pre-stretch tape diameter	-	94	mm
Post-stretch tape diameter 2	-	210	mm
Pre-stretch tape thickness	-	1	mm
Post-stretch tape thickness	z_0	200	µm
Internal plate radius	r	25	mm
External plate outer diameter	-	210	mm
External plate inner diameter	-	180	mm
Electrode width	l_0	65	mm

The obtained data were used to identify the value of Young's modulus in the developed FEM model. Figure 3 shows the membrane's FEM model loaded with force 1.42 [N]. Table 3 and Figure 4 provide a faithful comparison of simulations with measurements in the full load range of the actuator.

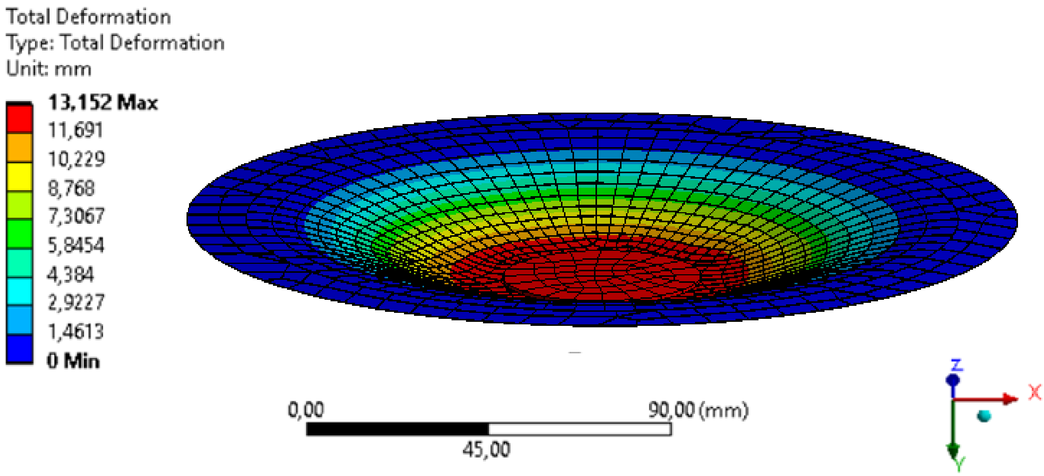

Figure 3. The finite element model (FEM) simulation of dielectric electro active polymer actuator for static force 1,42 [N].

Table 3. The comparison of the displacements for different load force.

Force [N]	Displacement Measurement [mm]	Displacement Model [mm]
0.00	0.00	0
0.64	6.83	5.93
1.03	10.37	9.54
1.23	12.08	11.39
1.42	13.48	13.15
1.67	15.80	15.46
1.98	18.42	18.33
2.10	19.34	19.44
2.22	20.50	20.56
2.33	21.29	21.57
2.45	22.27	22.69
2.61	23.55	24.17
2.77	24.95	25.65
2.92	26.48	27.04

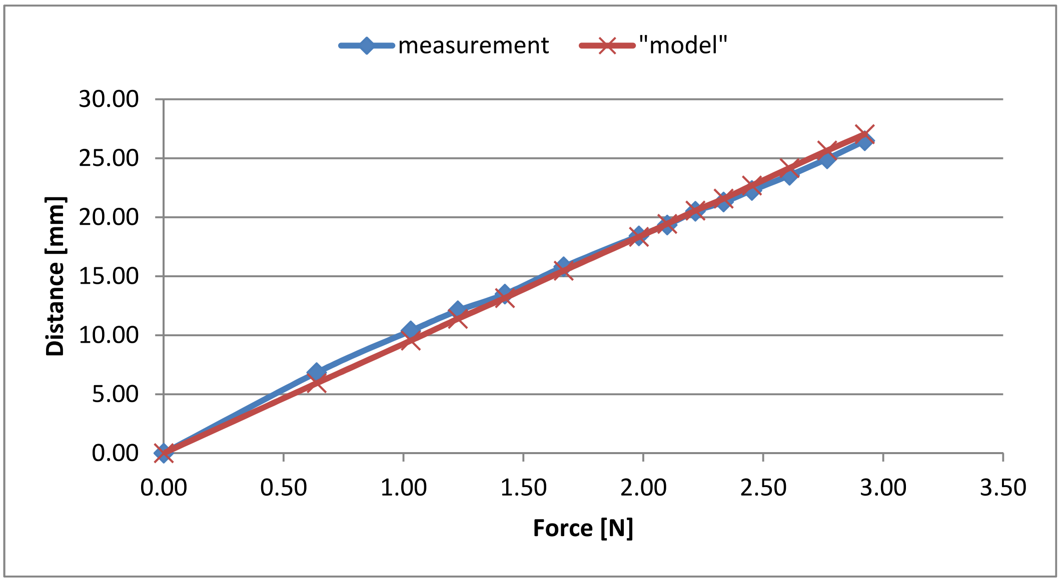

Figure 4. Comparison of membrane distances for different load forces.

3.2. The Identification Process

The operation of the device in an actuator mode using the DEAP membrane requires a power supply. To collect reference data, a number of experiments on the deformation of the actuator membrane were carried out under the influence of various supply voltages. The relatively narrow range of membrane supply was sampled at nine points from 5.0 [kV] to 7.0 [kV] with a 0.25 [kV] step. This approach allowed the determination of the virtual value of Young's modulus compensating for the nonlinear structure of the DEAP model.

To verify the correctness of the actuator modelling methodology, measurements were made for three different forces acting on the actuator. Tables 4–6 show the results of measurements and simulations carried out respectively for loads 1.03 [N], 1.23 [N] and 1.42 [N]. Figures 5–7 demonstrate the obtained convergence of the model with experimental measurements for the mentioned values of forces.

Table 4. The comparison of the displacements for different voltage supply and load force 1.03 [N].

Voltage Supply [kV]	Displacement Measurement [mm]	Displacement Model [mm]	Virtual Young Modulus [MPa]
5.00	12.02	12.08	7100
5.25	12.39	12.36	6950
5.50	12.80	12.76	6700
5.75	13.23	13.25	6450
6.00	13.76	13.71	6250
6.25	14.33	14.28	6000
6.50	15.00	15.03	5700
6.75	15.73	15.73	5450
7.00	16.56	16.56	5150

Table 5. The comparison of the displacements for different voltage supply and load force 1.23 [N].

Voltage Supply [kV]	Displacement Measurement [mm]	Displacement Model [mm]	Virtual Young Modulus [MPa]
5.00	14.12	14.06	7300
5.25	14.51	14.43	7100
5.50	14.96	14.88	6900
5.75	15.51	15.52	6625
6.00	16.09	16.06	6400
6.25	16.78	16.83	6075
6.50	17.51	17.50	5850
6.75	18.39	18.39	5575
7.00	19.33	19.26	5300

Table 6. The comparison of the displacements for different voltage supply and load force 1.42 [N].

Voltage Supply [kV]	Displacement Measurement [mm]	Displacement Model [mm]	Virtual Young Modulus [MPa]
5.00	16.47	16.47	7200
5.25	16.90	16.87	6975
5.50	17.43	17.34	6775
5.75	18.00	18.02	6600
6.00	18.76	18.8	6300
6.25	19.60	19.58	6050
6.50	20.40	20.35	5800
6.75	21.30	21.40	5550
7.00	22.40	22.24	5300

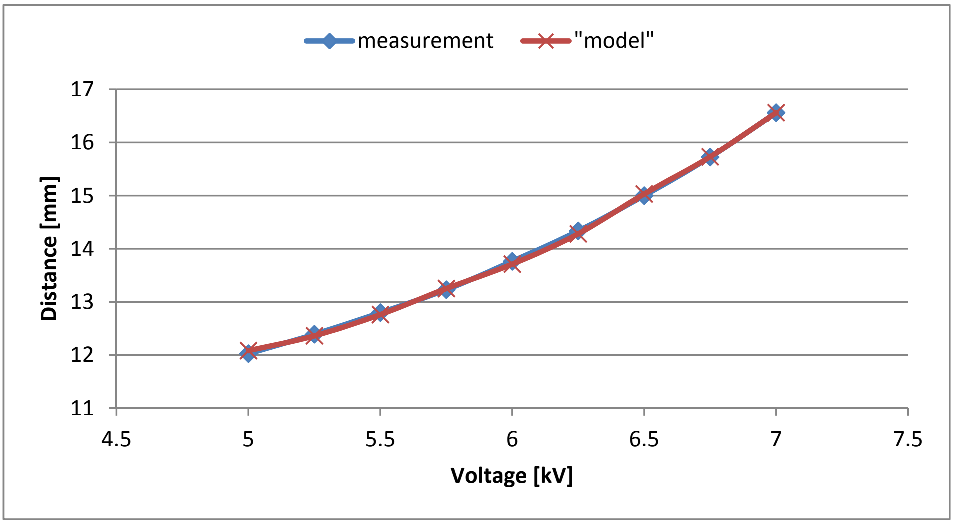

Figure 5. Comparison of membrane distances for static load force 1.03 [N].

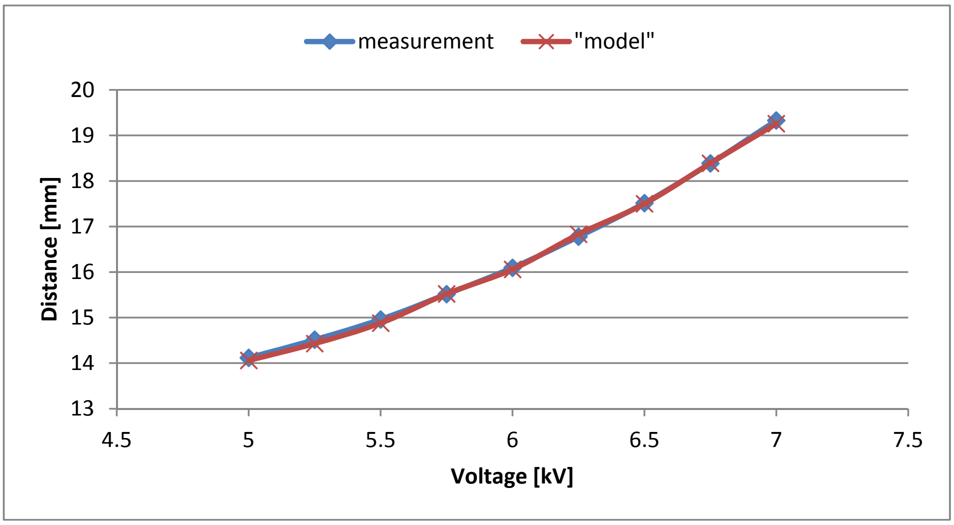

Figure 6. Comparison of membrane distances for static load force 1.23 [N].

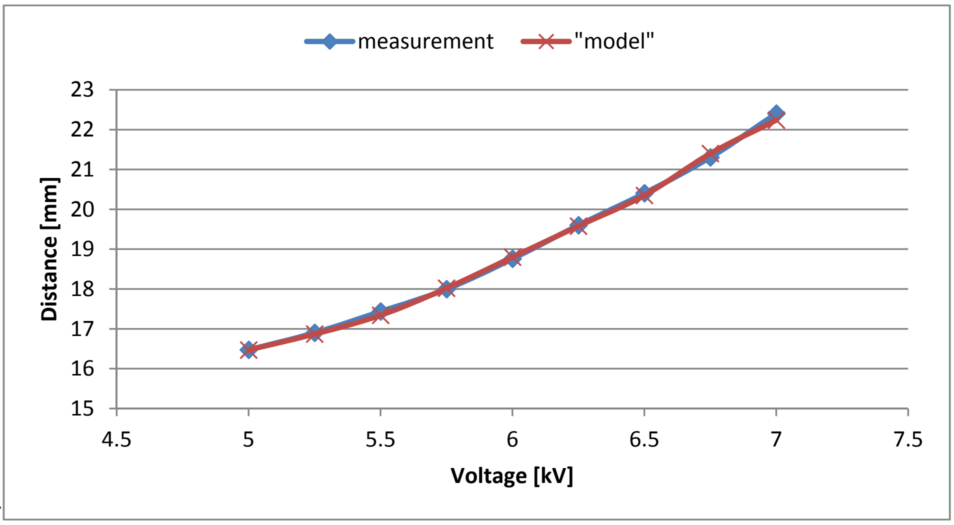

Figure 7. Comparison of membrane distances for static load force 1.42 [N].

The results of these experiments show that the parameters obtained from the voltage test sufficiently accurately describe the behavior of the membrane and can be used in the model.

4. Pump FEM Model with DEAP Membrane

Based on the obtained values of the virtual Young's module, a pump model was developed. In order to increase the force and thus the scope of the pump operation, two permanent magnets were implemented (see Figure 8). The model used neodymium magnets with a diameter of 17 [mm] and a height of 2 [mm]. The mass of each magnets was 3.4 [g] and the lifting capacity was about 2 [kg] for the induction of remanence 1.22–1.25 [T]. The force between two identical cylindrical magnets was approximately calculated according to Gilbert's model [17,18]. This force in the start position without the pump supply was 0.8 [N], which caused a static deformation of membranes equal to 8 [mm].

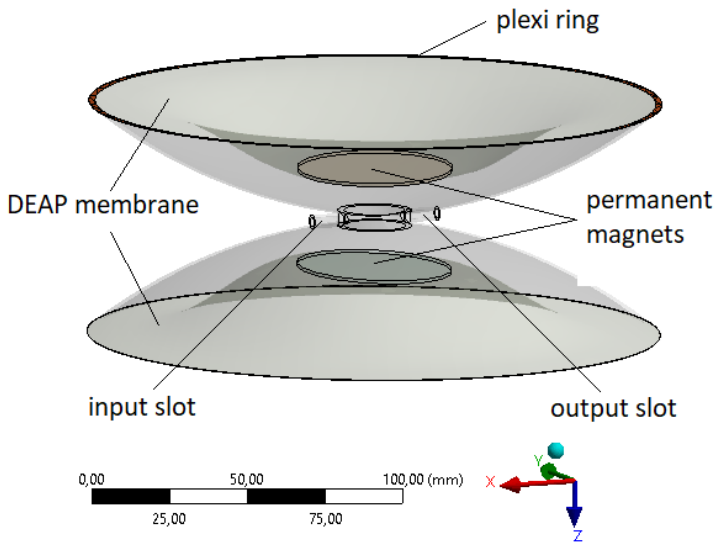

Figure 8. A pump concept built using a DEAP membrane and permanent magnets.

A pump chamber was proposed (see Figure 9), which is a segment of a sphere with a radius of 9 [cm].

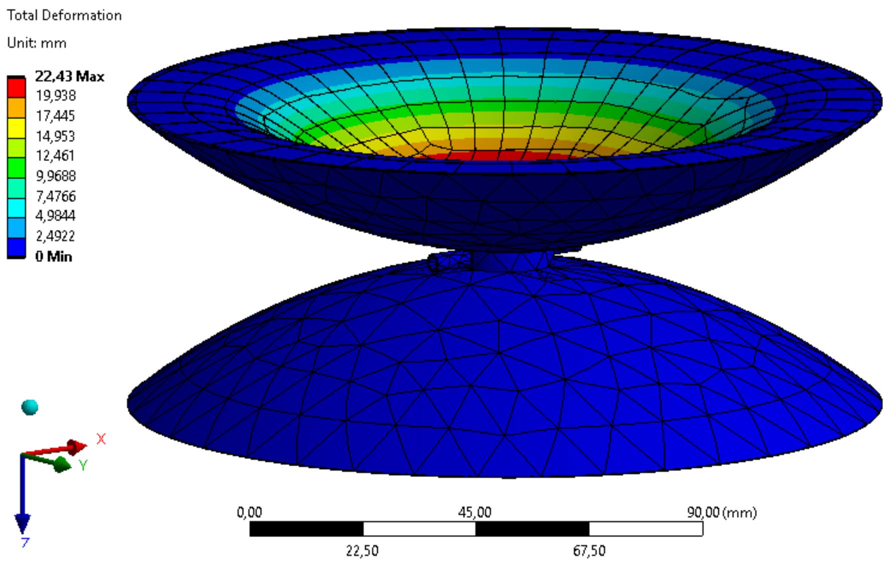

Figure 9. *Cont.*

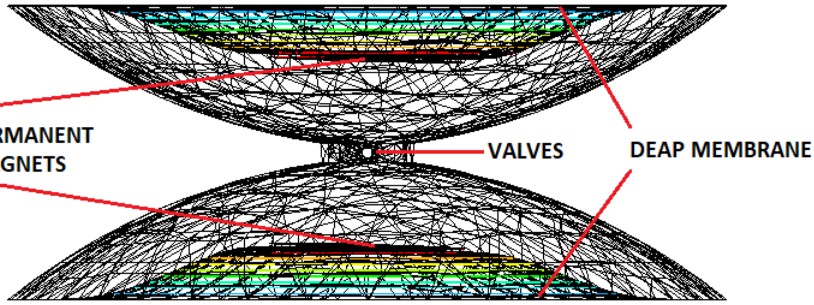

Figure 9. A pump concept built using a DEAP membrane and permanent magnets.

The boundary conditions applied in ANSYS software closely match the boundary conditions during the experiments. In the experiments the frame of the DEAP was clamped rigidly and the force was applied at the central part of the actuator. The actuator was designed to move out of plane by adding a fixed boundary constraint to the perimeter of the material. The scheme of the applied forces and the mechanical boundary conditions applied in ANSYS are as shown in the Figure 10.

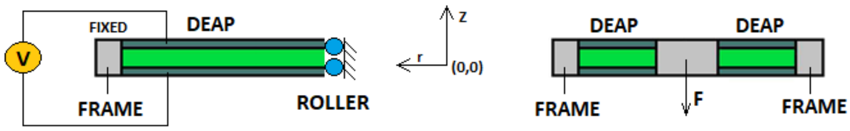

Figure 10. Mechanical Boundary conditions for experiments and ANSYS Environment.

Since, the outer plastic frame was rigid as compared to the elastomer, the outer end of the elastomer could be considered fixed to a rigid frame. Similarly, the circular part of the frame at the center of the EAP was rigid and hence no radial displacement of the polymer occurs at the inner end. The force was applied at the inner boundary in the vertically downward direction. For electromechanical simulations, the area surrounding the EAP was specified as air. The directional distribution of forces attracting magnets is shown in the Figure 11.

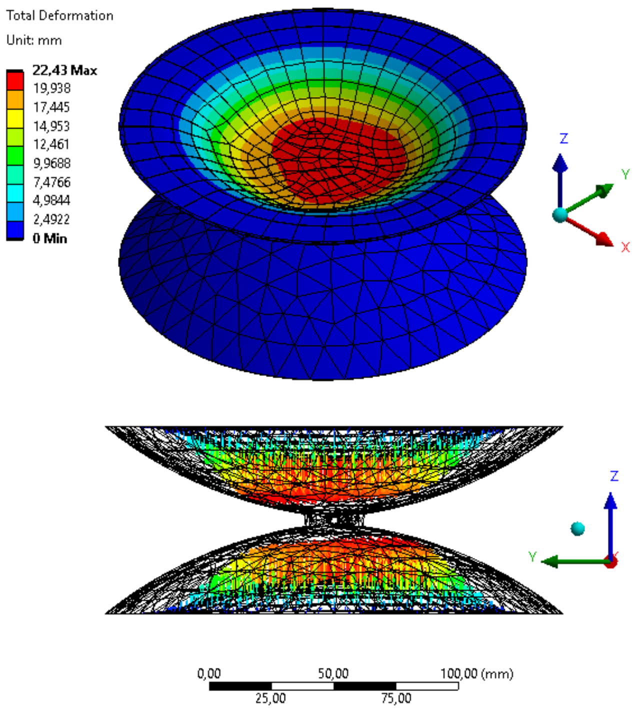

Figure 11. A grid view in the FEM model and distribution of force vectors.

In the suction cycle, the inlet slot (valve) opens and the outlet slot (valve) closes. In order to pump out the medium, the valves change their state and a voltage of 7 [kV] is applied to the membranes. The change in volume of one pump chamber ranges from 135.64 cm^3 to 379.81 cm^3 and its graph over time is shown in Figure 12. In the suction cycle, the inlet valve opens, and the outlet valve closes. In order to pump out the liquid, the valves change their state and the voltage on the membrane electrodes is switched on.

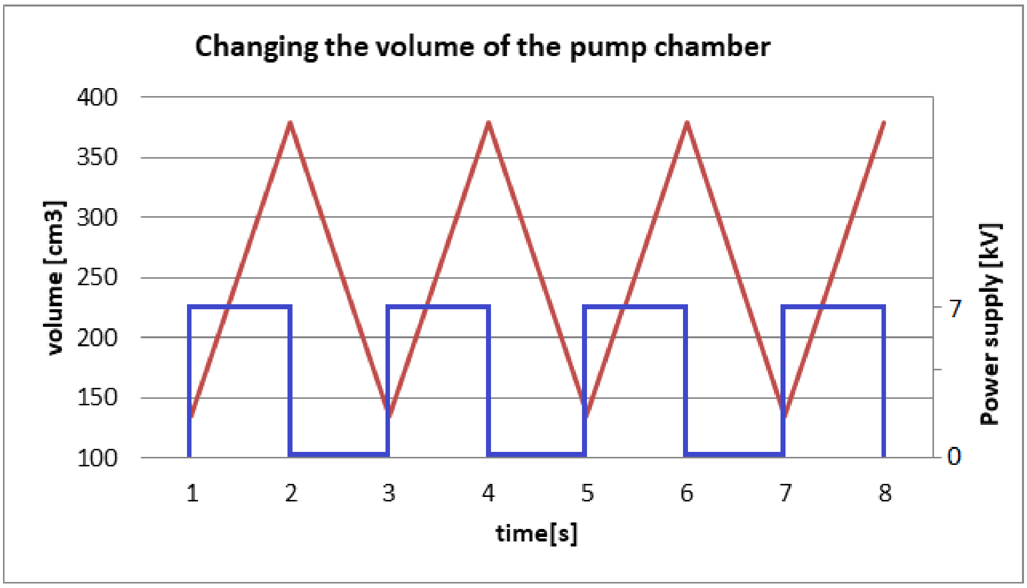

Figure 12. Supply voltage waveform and volume change of one pump chamber.

5. Conclusions

DEAPs are a subclass of electroactive polymers in which actuation is produced by an elastic deformation resulting from the compressive electrostatic forces. Their most important advantages like energy efficiency, lightweight and scalability are key features for actuators in applications such as pumps. Dielectric electroactive polymer technology is able to fulfill requirements as well as commonly used technology e.g., solenoids, but its limitations concern relatively low force [19,20]. One way to increase force generated by these devices can be the application of neodymium permanent magnets. The concept for pump presented in this paper consists of a stack of DEAP membranes combined with a permanent magnets. These two components are combined in a novel pump construction, which allows a compact design by integrating the biasing mechanism with the DEAP membranes. Subsequently, the single components are manufactured, tested, and their force-displacement characteristic is documented. Identifying the parameters experimentally allowed to develop a faithful FEM model of the pump device and make its simulations for different voltage. FEM modeling of the DEAP membrane behavior is a useful tool to understand such systems better and helps to create the optimal design of prototypes. These modeling efforts must account for the electromechanical coupling in order to accurately predict their response to multiple loading conditions expected during real operating conditions. Because of the complexity of the nonlinear processes, the finite element analysis is reasonable to be used and study the behaviour of dielectric elastomer pump. The experiments under static and transient considerations have been performed to validate the design and implementation. It is shown, that the model is in close agreement with the measured responses of the real DEAP actuator. The collected data allow for the analysis of various other device designs using DEAP membrane in the future.

Funding: This research was funded by NATIONAL SCIENCE CENTRE (Poland), project SONATA13 grant number No. 2017/26/D/ST7/00092. The APC was funded by NATIONAL SCIENCE CENTRE (Poland).

Conflicts of Interest: The author declare no conflict of interest.

References

1. Kim, K.J.; Tadokoro, S. *Electroactive Polymers for Robotics Applications: Artifical Muscles and Sensors*; Springer: London, UK, 2007. [CrossRef]
2. Bar-Cohen, Y. *Electroactive Polymer (EAP) Actuators as Artificial Muscles: Reality, Potential, and Challenges*; SPIE Press: Bellingham, DC, USA, 2001.
3. Carpi, F.; Anderson, I.; Bauer, S.; Frediani, G.; Gallone, G.; Gei, M.; Graaf, C.; Jean-Mistral, C.; Kaal, W.; Kofod, G.; et al. Standards for dielectric elastomer transducers. *Smart Mater. Struct.* **2015**, *24*. [CrossRef]
4. Berselli, G.; Vertechy, R.; Babi, M.; Castelli, V.P. Dynamic modeling and experimental evaluation of a constant-force dielectric elastomer actuator. *J. Intell. Mater. Syst. Struct.* **2013**, *24*, 779–791. [CrossRef]
5. Rosenblatt, F.; Morrison, J.F.; Iannuci, L. Modelling Electroactive Polymer (EAP) Actuators: Electro-Mechanical Coupling using Finite Element Software. In Proceedings of the SPIE Smart Structures and Materials + Nondestructive Evaluation and Health Monitoring, San Diego, CA, USA, 9–13 March 2008. [CrossRef]
6. Wissler, M.; Mazza, E. Electromechanical Coupling in Dielectric Elastomer Actuators. *Sens. Actuators A Phys.* **2007**, *138*, 384–393. [CrossRef]
7. He, T.; Zhao, X.; Suo, Z. Dielectric elastomer membranes undergoing inhomogeneous deformation. *J. Appl. Phys.* **2009**, *106*. [CrossRef]
8. Wang, S.; Decker, M.; Henann, D.L.; Chester, S.A. Modeling of dielectric viscoelastomers with application to electromechanical instabilities. *J. Mech. Phys. Solids* **2016**, *95*, 213–229. [CrossRef]
9. Li, Y.; Oh, I.; Chen, J.; Zhang, H.; Hu, Y. Nonlinear dynamic analysis and active control of visco-hyperelastic dielectric elastomer membrane. *Int. J. Solids Struct.* **2018**. [CrossRef]
10. Rosset, S.; Araromi, O.A.; Schlatter, S.; Shea, H. Fabrication process of silicone-based dielectric elastomer actuators. *J. Vis. Exp.* **2016**, *108*, 1–13. [CrossRef] [PubMed]
11. Rizzello, G.; Naso, D.; York, A.; Seelecke, S. Modeling, identification, and control of a dielectric electro-active polymer positioning system. *IEEE Trans. Control. Syst. Technol.* **2015**, *23*, 632–643. [CrossRef]
12. Wang, Z.; He, T. Electro-viscoelastic behaviors of circular dielectric elastomer membrane actuator containing concentric rigid inclusion. *Appl. Math. Mech.* **2018**, *39*, 547–560. [CrossRef]
13. De Saint-Aubin, C.; Rosset, S.; Schlatter, S.; Shea, H. High-cycle electromechanical aging of dielectric elastomer actuators with carbon-based electrodes. *Smart Mater. Struct.* **2018**, *27*. [CrossRef]
14. Hodgins, M.; Rizzello, G.; York, A.; Seelecke, S. High-frequency dynamic model of a pre-loaded circular dielectric electro-active polymer actuator. In Proceedings of the ASME 2013 Conference on Smart Materials, Adaptive Structures and Intelligent Systems, Snowbird, UT, USA, 16–18 September 2013. [CrossRef]
15. Bernat, J.; Kołota, J. Adaptive Controller with Output Feedback for Dielectric Electro-Active Polymer Actuator. In Proceedings of the 12th International Workshop on Robot. Motion and Control (RoMoCo'19), Poznań, Poland, 8–10 July 2019; pp. 247–251. [CrossRef]
16. Bernat, J.; Kołota, J. Adaptive Observer for State and Load Force Estimation for Dielectric Electro-Active Polymer Actuator. In Proceedings of the 11th IFAC Symposium on Nonlinear Control Systems NOLCOS 2019, Vienna, Austria, 4–6 September 2019.
17. Ravaud, R.; Lemarquand, G.; Babic, S.; Lemarquand, V.; Akyel, C. Cylindrical Magnets and Coils: Fields, Forces, and Inductances. *IEEE Trans. Magn.* **2010**, *46*, 3585–3590. [CrossRef]
18. Vokoun, D.; Beleggia, M.; Heller, L.; Sittner, P. Magnetostatic interactions and forces between cylindrical permanent magnets. *J. Magn. Magn. Mater.* **2009**, *21*, 3758–3763. [CrossRef]
19. Kaal, W.; Herold, S. Electroactive polymer actuators in dynamic applications. *IEEE/ASME Trans. Mechatron.* **2011**, *16*, 24–32. [CrossRef]
20. Anderson, I.; Gisby, T.; McKay, T.; O'Brien, B.; Calius, E. Multifunctional dielectric elastomer artificial muscles for soft and smart machines. *J. Appl. Phys.* **2012**, *112*. [CrossRef]